

# Tetranuclear Heterometallic Iron(II)–Lithium Carboxylates Stabilized by N-Donor Ligands: Synthesis and Structure

D. S. Yambulatov<sup>a</sup>, J. K. Voronina<sup>a</sup>, S. A. Nikolaevskii<sup>a, \*</sup>, A. I. Poddel'skii<sup>a</sup>,  
M. A. Kiskin<sup>a</sup>, and I. L. Eremenko<sup>a</sup>

<sup>a</sup> Kurnakov Institute of General and Inorganic Chemistry, Russian Academy of Sciences, Moscow, Russia

\*e-mail: sanikol@igic.ras.ru

Received November 21, 2022; revised December 2, 2022; accepted December 7, 2022

**Abstract**—The multicomponent chemical reactions of  $\text{Fe}(\text{SO}_4) \cdot 7\text{H}_2\text{O}$ ,  $\text{Li}(\text{Piv})$ ,  $\text{K}(\text{Piv})$  ( $\text{Piv}$  is pivalate anion), and heterocyclic N-donor ligands (pyridine (Py), 1,10-phenanthroline (Phen)) in anhydrous acetonitrile under an inert atmosphere afford new heterometallic tetranuclear complexes  $[\text{Fe}_2^{\text{II}}\text{Li}_2(\text{Piv})_6(\text{Py})_4]$  (**I**) and  $[\text{Fe}_2^{\text{II}}\text{Li}_2(\text{Piv})_6(\text{Phen})_2]$  (**II**) in which all carboxylate anions act as bridging ligands. The molecular and crystal structures of the compounds are determined by X-ray diffraction (XRD) (CIF files CCDC nos. 2220576 (**I**) and 2220577 (**II**·2CH<sub>3</sub>CN)). In the studied complexes, the iron(II) atoms exist in the distorted octahedral ligand environment.

**Keywords:** pivalate, tetranuclear complex, iron(II), lithium, XRD

**DOI:** 10.1134/S1070328423600250

## INTRODUCTION

Heterometallic coordination and metal-organic compounds containing iron and lithium atoms in one molecule became popular objects of research. They are characterized by rich structural chemistry [1–4] and promising functional properties [5–8], which can be controlled, to some extent, by the variation of the steric and electronic characteristics of the bridging ligands and by switching over oxidation states of the iron ion. Among the most nonstandard areas of the potential application of the Fe–Li compounds, one can emphasize their use as metallating agents capable of selectively detaching protons in partially substituted fluoroarenes [9]. The Fe–Li compounds are most frequently studied as promising precursors for manufacturing cathodes for Li-ion batteries [10] and structural analogs of inorganic perovskites [11] or frustrated magnetic phases [12].

Carboxylate ligands are convenient polyfunctional platforms for the preparation and study of new polynuclear architectures [13–25] including those built due to binding RCOO groups with iron and lithium cations [26–29]. Although polynuclear heterometallic carboxylates bearing *s*- and *d*-metal atoms are studied rather intensely [30–37], we succeeded to find only 19 structurally characterized Fe–Li carboxylate complexes in the Cambridge Structural Database (version 5.43, updated on March 2022). The main problem for synthetic chemists working in this area is the affinity of iron(II) ions to oxidative hydrolysis [38] leading to the formation of complex oxides and hydroxides [26, 39, 40].

In this work, we present the results on the synthesis and study of the structures of the heterometallic Fe(II)–Li(I) pivalate complexes with the tetranuclear  $\{\text{Fe}_2\text{Li}_2\}$  metal core stabilized by the coordination of the neutral N-donor ligands (pyridine (Py) and 1,10-phenanthroline (Phen)).

## EXPERIMENTAL

The target products were synthesized and isolated in an inert atmosphere using the standard Schlenk technique. Acetonitrile (reagent grade, Khimmed) was dried over phosphorus(V) oxide, stored over activated molecular sieves (4 Å), and taken using condensation prior to synthesis. Lithium and potassium pivalates were synthesized using known procedures [41, 42]. Prior to the reaction with iron(II) sulfate, potassium pivalate was heated at 140°C in an oil bath for a day in a dynamic vacuum. Iron(II) pivalate  $[\text{Fe}(\text{Piv})_2]$ , was synthesized by the exchange reaction from  $\text{Fe}(\text{SO}_4) \cdot 7\text{H}_2\text{O}$  and  $\text{KPiv}$  in degassed ethanol without air access with stirring at room temperature for 3 days. The formed precipitate of potassium sulfate was filtered off after the solvent was replaced by acetonitrile and a pyridine excess or an equimolar amount of 1,10-phenanthroline was added to form soluble iron complexes of the assumed composition  $[\text{Fe}_2(\text{Piv})_4(\text{Py})_2]$  or  $[\text{Fe}(\text{Piv})_2(\text{Phen})]$  [43]. Commercially available lithium hydroxide  $\text{LiOH} \cdot \text{H}_2\text{O}$  and potassium acetate (reagent grade, Ruskhim),  $\text{Fe}(\text{SO}_4) \cdot 7\text{H}_2\text{O}$ , pyridine (reagent grade, Khimmed), HPiv (reagent grade, Alfa

Aesar), and Phen (reagent grade, Aldrich) were used as received.

IR spectra were recorded in a range of 400–4000 cm<sup>−1</sup> on a Perkin Elmer Spectrum 65 spectrophotometer equipped with a Quest ATR Accessory instrument (Spectac) by the attenuated total internal reflectance (ATR) method. Elemental analysis was carried out on a EuroEA-3000 C,H,N,S analyzer (EuroVektor).

**Synthesis of  $[\text{Fe}_2\text{Li}_2(\text{Piv})_6(\text{Py})_4]$  (I).** A weighed sample of lithium pivalate (0.108 g, 1.0 mmol) was placed in a glass ampoule and degassed in a dynamic vacuum for 10 min. Acetonitrile (10 mL) was condensed to iron(II) pivalate, which was in situ prepared from  $\text{Fe}(\text{SO}_4) \cdot 7\text{H}_2\text{O}$  (0.254 g, 1.0 mmol) and KPiv (0.280 g, 2.0 mmol), and a pyridine excess (1 mL, 12.5 mmol) was added. The reaction mixture was filtered from potassium sulfate, and the yellow filtrate was poured to lithium pivalate. The ampoule was sealed and heated in an oil bath at 110°C for 8 h to the complete dissolution of lithium pivalate and formation of a transparent yellow solution. The further cooling of the reaction mixture and holding at −18°C for 24 h gave yellow crystals. The yield was 0.382 g (73%).

For  $\text{C}_{50}\text{H}_{74}\text{N}_4\text{O}_{12}\text{Li}_2\text{Fe}_2$

Anal. calcd., %	C, 57.26	H, 7.11	N, 5.34
Found, %	C, 57.22	H, 7.01	N, 5.28

IR (ATR;  $\nu$ , cm<sup>−1</sup>): 2958 m, 2915 w, 2864 w, 1579 s, 1557 s, 1481 s, 1444 m, 1409 vs, 1359 s, 1224 s, 1152 w, 1071 w, 1033 w, 1005 w, 939 w, 898 m, 791 m, 754 m, 701 m, 603 m, 559 w, 409 vs.

**Synthesis of  $[\text{Fe}_2\text{Li}_2(\text{Piv})_6(\text{Phen})_2] \cdot 2(\text{CH}_3\text{CN})$  (II·2CH<sub>3</sub>CN).** A weighed sample of lithium pivalate (0.108 g, 1.0 mmol) was placed in a glass ampoule and degassed in a dynamic vacuum for 10 min. Acetonitrile (10 mL) was condensed to iron(II) pivalate, which was prepared in situ from  $\text{Fe}(\text{SO}_4) \cdot 7\text{H}_2\text{O}$  (0.254 g, 1.0 mmol) and KPiv (0.280 g, 2.0 mmol), and Phen was added. The orange reaction mixture was filtered from potassium sulfate, and the filtrate was poured to lithium pivalate. The ampoule was sealed and heated in an oil bath at 110°C for 10 h. The further cooling to room temperature gave green crystals. The yield was 0.493 g (84%).

For  $\text{C}_{58}\text{H}_{76}\text{N}_6\text{O}_{12}\text{Li}_2\text{Fe}_2$

Anal. calcd., %	C, 59.30	H, 6.52	N, 7.15
Found, %	C, 59.21	H, 6.34	N, 7.09

IR (ATR;  $\nu$ , cm<sup>−1</sup>): 3062 w, 2958 m, 2918 m, 2867 m, 2253 w, 1576 vs, 1481 s, 1406 vs, 1359 s, 1224 s, 1146 w, 1096 w, 1030 w, 933 w, 892 m, 845 m, 795 m, 723 m, 600 s, 556 m, 434 vs, 421 vs, 403 vs.

**XRD** of single crystals of the studied compounds was carried out on a Bruker D8 Venture automated diffractometer equipped with a CCD detector (graphite monochromator,  $\text{MoK}_\alpha$  radiation,  $\lambda = 0.71073 \text{ \AA}$ ,

$\omega$  and  $\phi$  scan modes) at 100 K. An absorption correction was applied semiempirically using the SADABS program [44]. The structures were solved and refined first in the isotropic approximation and then in the anisotropic approximation by the SHELXL-2018/3 program [45] using OLEX2 [46]. Hydrogen atoms were placed in geometrically calculated positions and included into refinement by the riding model. The crystallographic parameters and structure refinement details are given in Table 1.

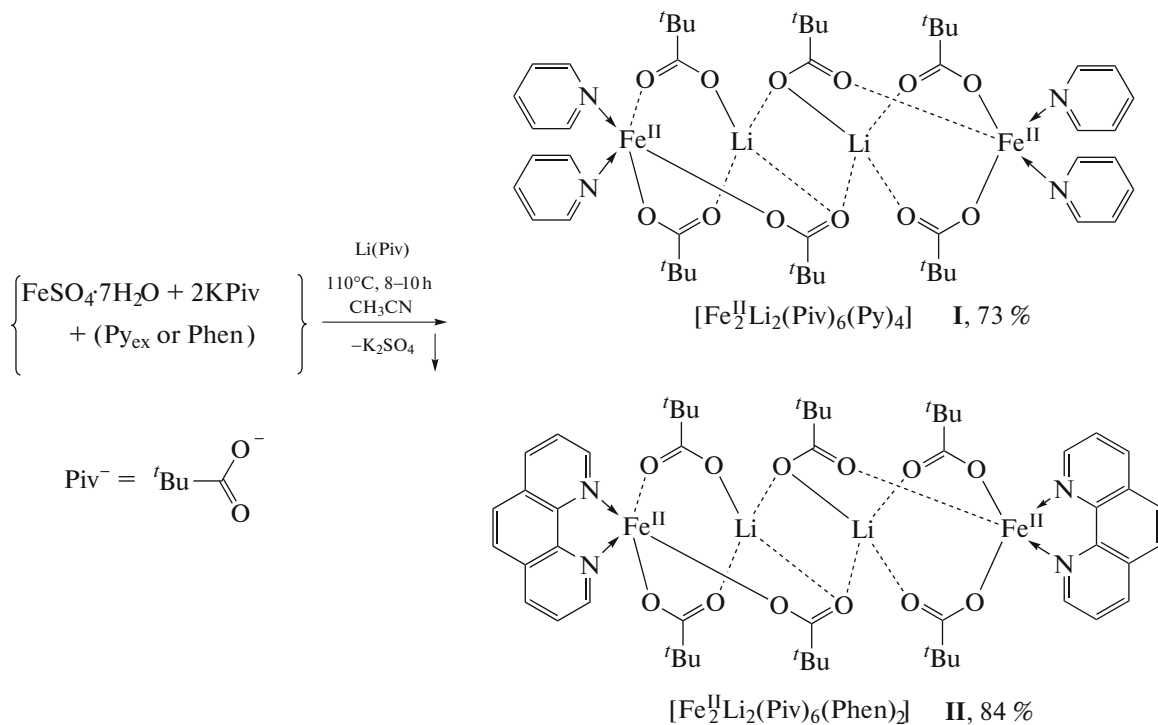
The full set of XRD parameters for the structures of compounds **I** and **II**·2CH<sub>3</sub>CN was deposited with the Cambridge Crystallographic Data Centre (CIF files CCDC nos. 2220576 and 2220577, respectively; deposit@ccdc.cam.ac.uk or [http://www.ccdc.cam.ac.uk/data\\_request/cif](http://www.ccdc.cam.ac.uk/data_request/cif)).

## RESULTS AND DISCUSSION

The polynuclear complexes  $[\text{Fe}_2^{\text{II}}\text{Li}_2(\text{Piv})_6(\text{Py})_4]$  (**I**) and  $[\text{Fe}_2^{\text{II}}\text{Li}_2(\text{Piv})_6(\text{Phen})_2]$  (**II**) were synthesized by the reactions of the corresponding iron(II) pivalate complexes with the nitrogen-containing base (Py or Phen) and lithium pivalate at 110°C for 8–10 h in an acetonitrile solution (Scheme 1).

The complexes were isolated from the reaction mixture after cooling as yellow (**I**) and green (**II**) single crystals. The structures of compounds **I** and **II** were determined by XRD (Fig. 1). In the crystal, the molecules of the complexes are centrosymmetric, and the crystal cell of complex **I** contains two crystallographically independent molecules. The crystals of compound **II** contain two solvate acetonitrile molecules per molecule of the complex.

In both complexes, the central Fe(1) iron atoms are in the distorted octahedral ligand environment formed by four oxygen atoms of three pivalate ligands and two nitrogen atoms of the terminal donor ligands (two Py or Phen, respectively), and the Li(1) lithium ions exist in the weakly distorted tetrahedral environment of four oxygen atoms of the carboxyl groups (Fig. 2). Note that the metal core is formally described as  $\{\text{Fe}_4\text{Li}_2\text{O}_2\}$  in the previously studied polynuclear Fe(III)–Li oxocarboxylates. This metal core contains bridging carboxylates of three different types (six  $O,O'$ - $\mu^2$ -, two  $O,O$ - $\mu^2$ -, and two  $O,O,O'$ - $\mu^3$ -carboxylates) and is close in structure to the structures of other known hexapolynuclear carboxylates of the  $[\text{M}'_2\text{M}''_4(\text{O})_2(\text{O}_2\text{CR})_{10}\text{L}_4]$  type ( $\text{M}' = \text{Fe}(\text{III}), \text{Mn}(\text{III})$ ;  $\text{M}'' = \text{Mn}(\text{II}), \text{Fe}(\text{II}), \text{Co}(\text{II}), \text{Ni}(\text{II})$  [47–49]). Unlike the mentioned oxocarboxylates, the metallic cage of complexes **I** and **II** is described by the  $\{\text{Fe}_2\text{Li}_2\}$  composition and contains pivalate ligands of two types: two  $O,O'$ - $\mu^2$ - and four  $O,O,O'$ - $\mu^3$ -pivalates (in two of them the bridging oxygen atom binds two lithium atoms; in two others the bridging oxygen atom binds one iron atom and one lithium atom).



Scheme 1.

Table 1. Crystallographic data structure refinement parameters for compounds **I** and **II**

Parameter	Value	
	<b>I</b>	<b>II</b>
Empirical formula	$2(\text{C}_{50}\text{H}_{74}\text{N}_4\text{O}_{12}\text{Li}_2\text{Fe}_2)$	$\text{C}_{54}\text{H}_{70}\text{N}_4\text{O}_{12}\text{Li}_2\text{Fe}_2 \cdot 2(\text{C}_2\text{H}_3\text{N})$
<i>FW</i>	2097.42	1174.82
Crystal system, space system	Triclinic, $P\bar{1}$	Triclinic, $P\bar{1}$
<i>a</i> , Å	12.639(2)	11.9192(5)
<i>b</i> , Å	14.055(2)	12.0100(6)
<i>c</i> , Å	17.879(3)	12.4795(5)
$\alpha$ , deg	80.098(6)	61.385(1)
$\beta$ , deg	80.169(6)	79.953(2)
$\gamma$ , deg	67.402(6)	84.589(1)
<i>V</i> , Å <sup>3</sup>	2869.4(8)	1544.07(12)
<i>Z</i>	1	1
$\mu$ , mm <sup>-1</sup>	0.56	0.53
Crystal sizes, mm	0.15 × 0.11 × 0.02	0.18 × 0.15 × 0.11
<i>T</i> <sub>min</sub> , <i>T</i> <sub>max</sub>	0.271, 0.381	0.304, 0.381
Number of measured reflections	17003	23836
Number of independent reflections	9830	7796
Number of reflections with $I > 2\sigma(I)$	6993	6863
<i>R</i> <sub>int</sub>	0.052	0.036
<i>R</i> <sub>1</sub> /w <i>R</i> ( <i>F</i> <sup>2</sup> ), ( $I > 2\sigma(I)$ )	0.0845/0.2385	0.0320/0.0801
<i>R</i> <sub>1</sub> /w <i>R</i> ( <i>F</i> <sup>2</sup> ), (for all reflections)	0.1163/0.2598	0.0384/0.0833
Number of refined parameters	688	384
Residual electron density max/min, e Å <sup>-3</sup>	1.25, -1.06	0.54, -0.41

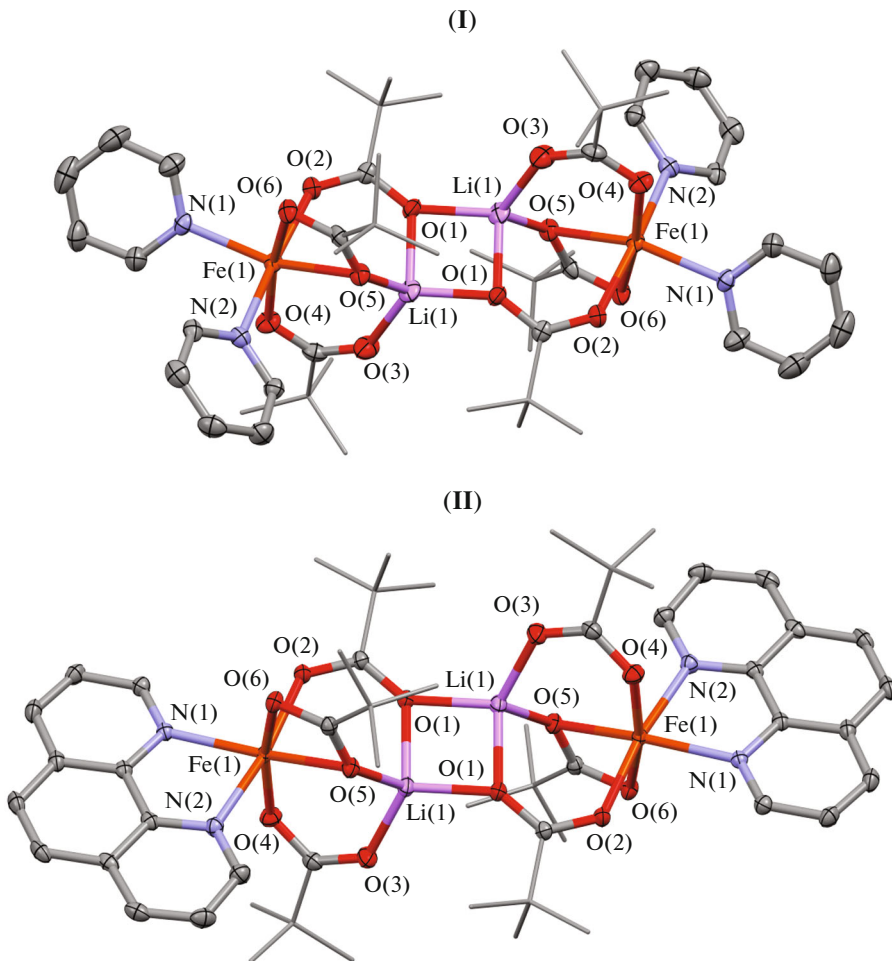


**Fig. 1.** Molecular structures of complexes **I** and **II** in the crystalline state according to the XRD data. Ellipsoids of 50% probability (carbon atoms of *tert*-butyl groups are shown without ellipsoids). Hydrogen atoms are omitted. Selected bond lengths (Å): Fe(1)–N(1) 2.158(5), Fe(1)–N(2) 2.161(5), Fe(1)–O(2) 2.129(4), Fe(1)–O(4) 2.027(4), Fe(1)–O(5) 2.252(4), Fe(1)–O(6) 2.178(4), Li(1)–O(1) 1.973(13), Li(1)–O(3) 1.881(11), Li(1)–O(5) 1.909(11), and Li(1)–O(1') 1.914(11) (**I**); Fe(1)–N(1) 2.159(1), Fe(1)–N(2) 2.190(1), Fe(1)–O(2) 2.078(1), Fe(1)–O(4) 2.020(1), Fe(1)–O(5) 2.236(1), Fe(1)–O(6) 2.232(1), Li(1)–O(1) 2.024(2), Li(1)–O(3) 1.915(2), Li(1)–O(5) 1.922(2), and Li(1)–O(1') 1.937(2) (**II**).

Thus, in both compounds, all carboxylate ligands are bridging and bind the iron Fe(1) and lithium Li(1) ions due to the oxygen atoms. The Fe(1)–O(2) and Fe(1)–O(4) bonds with nonbridging O atoms (2.129(4) and 2.027(4) Å in **I** and 2.078(1) and 2.020(1) Å in **II**) are somewhat shorter than the Fe(1)–O(5) bond with the bridging O atom (2.252(4) Å in **I** and 2.236(1) Å in **II**). On the one hand, these Fe–O bonds in complexes **I** and **II** are longer than those in the related polynuclear iron(III)–lithium pivalate complexes, for example,  $[\text{Fe}_3^{\text{III}}\text{Li}_2(\text{Piv})_{10}(\mu\text{-O})_2(\text{H}_2\text{O})_2]$  (1.988–2.063 Å) [28],  $[\text{Fe}_6^{\text{III}}\text{Li}_5(\text{'BuPO}_2)_6(\text{Piv})_8(\mu\text{-O})_2(\text{MeOH})_2]$  (1.96–2.05 Å) [1], which can be a result of a substantial

decrease in the electron density delocalization in the Fe–O–C=O carboxylate fragment compared to the usually delocalized carboxylate OCO fragment in the compounds with bridging or semibridging anions of carboxylic acids [50–52]. On the other hand, the Fe–O bonds correspond, on the average, to similar bonds in the polynuclear iron(II) carboxylate complexes, for instance, in  $[\text{Fe}_2^{\text{II}}\text{Li}_2(\text{L})_6]$  ( $\text{L} = \mu\text{-}tert\text{-butyl-3-oxybut-2-enoate}$ ) (2.04–2.22 Å) [53].

In the crystal of complex **I**, the molecules of the complex are linked with each other by the van der Waals and C–H...O interactions (Table 2). In the crystal of compound **II**, C–H...π and π...π interactions occur between the molecules of the complex along with intra- and intermolecular con-

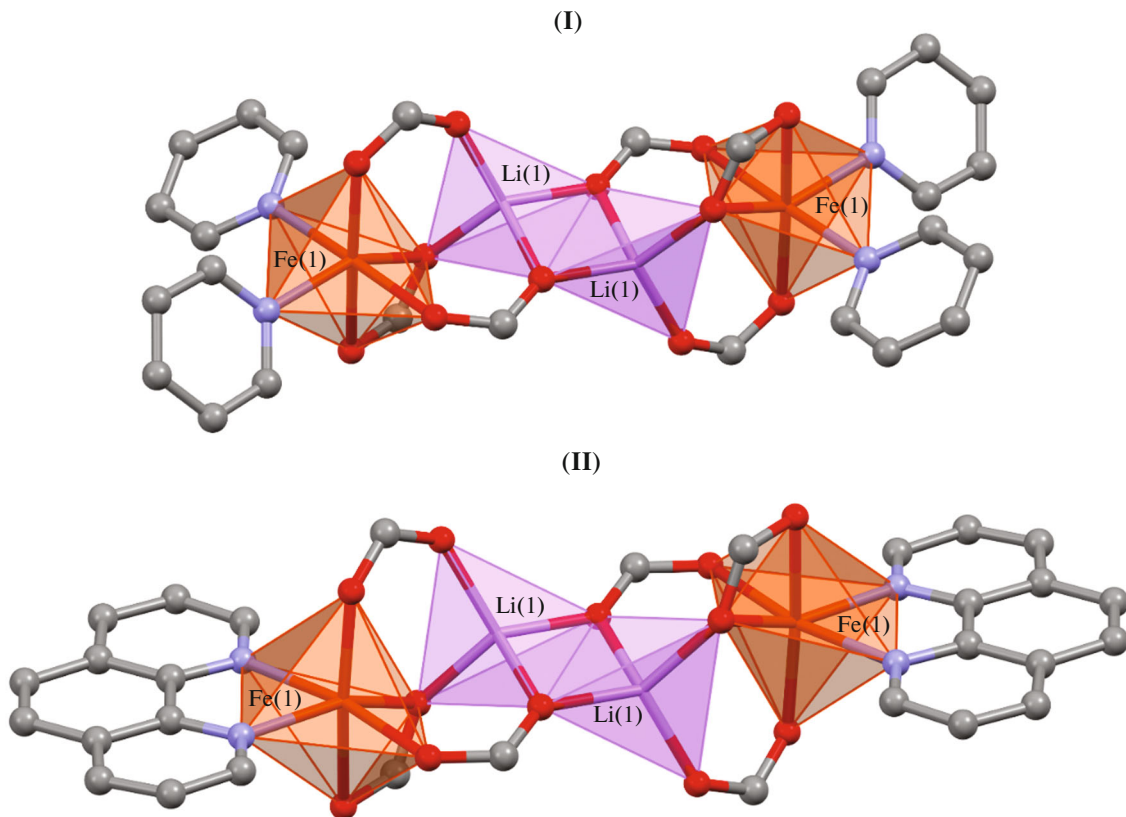


**Fig. 2.** Polyhedra  $\text{FeO}_4\text{N}_2$  and  $\text{LiO}_4$  in complexes **I** and **II**.

tacts C–H...O (Table 2). Stacking interactions between the pyridyl and phenyl cycles of the coordinated Phen molecules of the adjacent molecules are observed in the crystal resulting in the formation of a supramolecular chain (Fig. 3).

To conclude, we proposed new efficient methods for the synthesis of the earlier unknown molecular pivalates with iron(II) and lithium ions in a ratio of 2 : 2 (complexes **I** and **II**) in the yield higher than 70% and determined the molecular and crystal structures of these products. Note that the new iron(II) complexes with the  $\{\text{Fe}_2\text{Li}_2\}$  metal core supplement the series of

the known architectures with cobalt(II), nickel(II), copper(II), zinc(II), and cadmium(II) ions [54–56] and are interesting as objects of studying the magnetic and catalytic properties.

#### ACKNOWLEDGMENTS

XRD, elemental analysis, and IR spectroscopy were carried out using the equipment of the Joint Research Center of Physical Methods of Research at the Kurnakov Institute of General and Inorganic Chemistry (Russian Academy of Sciences).

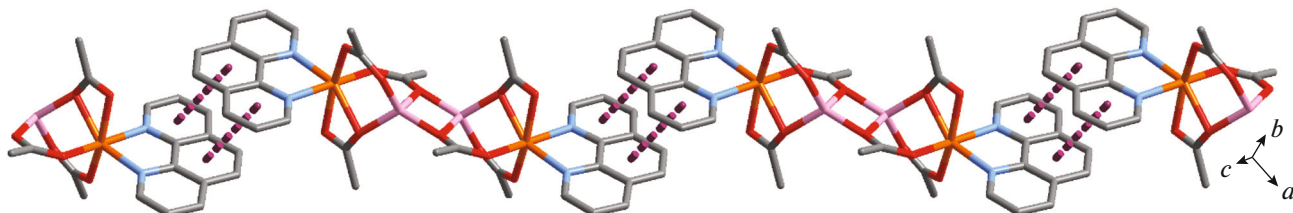


**Fig. 3.** Fragment of packing of the molecules of compound **II** in the crystal ( $\pi\cdots\pi$  interactions are shown by dash; H atoms, Me groups, and solvate molecules are omitted).

**Table 2.** Selected parameters of intra- and intermolecular interactions in compounds **I** and **II** (Cg is the aromatic ring centroid, H/C...Cg is the distance from the atom to the center of the cycle, C—H- $\pi$  is the angle between the C—H bond and plane of the cycle, Cg<sub>I</sub>—Cg<sub>J</sub> is the distance between the centroids of rings *I* and *J*,  $\alpha$  is the angle between the planes of the rings, Cg<sub>I</sub>\_perp is the distance defined as the perpendicular put from Cg<sub>I</sub> onto the plane of ring *J*, and Slippage is the distance between the Cg<sub>I</sub> and perpendicular projection of Cg<sub>J</sub> onto ring *I*)

Type of interaction	Parameters				
<b>I</b>					
C—H...A	Symmetry element	D—H, Å	H...A, Å	D...A, Å	Angle DHA, deg
C(24A)—H...O(6A)	$-x, 2 - y, 1 - z$	0.95	2.42	3.357(8)	169
C(24B)—H...O(2A)	$1 - x, 1 - y, 1 - z$	0.95	2.51	3.399(11)	155
<b>II</b>					
C—H...A	Symmetry element	D—H, Å	H...A, Å	D...A, Å	Angle DHA, deg
C(5)—H...O(3)	$x, y, z$	0.98	2.58	3.4922(19)	155
C(1S)—H...O(6)	$x, y, z$	0.98	2.44	3.079(2)	123
C(17)—H...O(4)	$-x, 1 - y, 1 - z$	0.95	2.57	3.4107(18)	147
C(24)—H...N(1S)	$x, y, 1 + z$	0.95	2.59	3.241(2)	126
C—H... $\pi$	Symmetry element	H...Cg, Å	C...Cg, Å	C—H—Cg, deg	$\gamma$ , deg
C(3)—H...Cg, where Cg is centroid of ring N(1)C(16)C(17)C(18)C(19)C(27)	$1 + x, y, z$	2.81	3.767(2)	166	9.36
$\pi$ ... $\pi$	Symmetry element	Cg <sub>I</sub> —Cg <sub>J</sub> , Å	$\alpha$ , deg	Cg <sub>I</sub> _perp, Å	$\gamma$ , deg
Cg <sub>I</sub> ...Cg <sub>J</sub> , where ring <i>I</i> is N(2)C(25)C(24)C(23)C(23)C(26), ring <i>J</i> is C(19)C(20)C(21)C(22)C(23)C(26)C(27)	$-x, -y, 2 - z$	3.7005(10)	0.89(8)	3.3190(7)	26.2

## FUNDING

This work was supported by the Russian Science Foundation, project no. 19-13-00436-P.

## CONFLICT OF INTEREST

The authors of this work declare that they have no conflicts of interest.

## REFERENCES

1. Khanra, S., Helliwell, M., Tuna, F., et al., *Dalton Trans.*, 2009, p. 6166.
2. Mund, G., Vidovic, D., Batchelor, R.J., et al., *Chem.-Eur. J.*, 2003, vol. 9, p. 4757.
3. Chen, C., Fröhlich, R., Kehr, G., and Erker, G., *Organometallics*, 2008, vol. 27, p. 3248.
4. Cross, R.J., Farrugia, L.J., McArthur, D.R., Peacock, R.D., and Taylor, D.S.C., *Inorg. Chem.*, 1999, vol. 38, p. 5698.
5. Subban, C.V., Ati, M., Rousse, G., et al., *J. Am. Chem. Soc.*, 2013, vol. 135, p. 3653.
6. Berben, L.A. and Long, J.R., *Inorg. Chem.*, 2005, vol. 44, p. 8459.
7. Scheibitz, M., Li, H., Schnorr, J., et al., *J. Am. Chem. Soc.*, 2009, vol. 131, p. 16319.
8. Martin, L., Engelkamp, H., Akutsu, H., et al., *Dalton Trans.*, 2015, vol. 44, p. 6219.
9. Maddock, L.C.H., Kennedy, A., and Hevia, E., *Chimia*, 2020, vol. 74, p. 866.
10. Yao, W., Armstrong, A.R., Zhou, X., et al., *Nat. Commun.*, 2019, vol. 10, p. 3483.
11. Clulow, R., Bradford, A.J., Lee, S.L., and Lightfoot, P., *Dalton Trans.*, 2019, vol. 48, p. 14461.
12. Yao, W., Clark, L., Xia, M., et al., *Chem. Mater.*, 2017, vol. 29, p. 6616.
13. Lutsenko, I.A., Yambulatov, D.S., Kiskin, M.A., et al., *Polyhedron*, 2021, vol. 206, e115354.
14. Adonin, S.A., Novikov, A.S., and Fedin, V.P., *Russ. J. Coord. Chem.*, vol. 46, p. 119.  
<https://doi.org/10.1134/S1070328420020013>

15. Nikolaevskii, S.A., Petrov, P.A., Sukhikh, T.S., et al., *Inorg. Chim. Acta*, 2020, vol. 508, e119643.
16. Sidorov, A.A., Kiskin, M.A., Aleksandrov, G.G., et al., *Russ. J. Coord. Chem.*, 2016, vol. 42, p. 621. <https://doi.org/10.1134/S1070328416100031>
17. Sidorov, A.A., Gogoleva, N.V., Bazhina, E.S., et al., *Pure Appl. Chem.*, 2020, vol. 92, p. 1093.
18. Adonin, S.A., Petrov, M.D., Novikov, A.S., et al., *J. Clust. Sci.*, 2019, vol. 30, p. 857.
19. Bondarenko, M.A., Novikov, A.S., Korolkov, I.V., et al., *Inorg. Chim. Acta*, 2021, vol. 524, e120436.
20. Bondarenko, M.A., Abramov, P.A., Novikov, A.S., et al., *Polyhedron*, 2022, vol. 214, e115644.
21. Bondarenko, M.A. and Adonin, S.A., *J. Struct. Chem.*, 2021, vol. 62, p. 1251. <https://doi.org/10.1134/S0022476621080114>
22. Zaguzin, A.S., Sukhikh, T.S., Kolesov, B.A., et al., *Polyhedron*, 2022, vol. 212, p. 115587.
23. Yoshinari, N. and Konno, T., *Coord. Chem. Rev.*, 2023, vol. 474, e214850.
24. Yambulatov, D.S., Nikolaevskii, S.A., Shmelev, M.A., et al., *Mendeleev Commun.*, 2021, vol. 31, p. 624.
25. Nikolaevskii, S.A., Yambulatov, D.S., Voronina, J.K., et al., *ChemistrySelect*, 2020, vol. 5, p. 12829.
26. Li, J.-H., Liu, H., Wei, L., and Wang, G.-M., *Solid State Sci.*, 2015, vol. 48, p. 225.
27. Lutsenko, I.A., Kiskin, M.A., Nikolaevskii, S.A., et al., *Mendeleev Commun.*, 2020, vol. 30, p. 273.
28. Lutsenko, I.A., Kiskin, M.A., Aleksandrov, G.G., et al., *Russ. Chem. Bull.*, 2018, vol. 67, p. 449. <https://doi.org/10.1007/s11172-018-2091-x>
29. Lutsenko, I.A., Kiskin, M.A., Tigai, Y.A., et al., *Russ. J. Coord. Chem.*, 2022, vol. 48, p. 760. <https://doi.org/10.1134/S1070328422110070>
30. Bazhina, E.S., Kiskin, M.A., Babeshkin, K.A., et al., *Inorg. Chim. Acta*, 2023, vol. 544, p. 121238.
31. Bazhina, E.S., Kiskin, M.A., Korlyukov, A.A., et al., *Eur. J. Inorg. Chem.*, 2020, vol. 2020, p. 4116.
32. Bazhina, E.S., Aleksandrov, G.G., Kiskin, M.A., et al., *Polyhedron*, 2017, vol. 137, p. 246.
33. Bazhina, E.S., Gogoleva, N.V., Zorina-Tikhonova, E.N., et al., *J. Struct. Chem.*, 2019, vol. 60, p. 855. <https://doi.org/10.1134/S0022476619060015>
34. Hursthouse, M.B., Light, M.E., and Price, D.J., *Angew. Chem., Int. Ed. Engl.*, 2004, vol. 43, p. 472.
35. Yao, R., Li, Y., Chen, Y., et al., *J. Am. Chem. Soc.*, 2021, vol. 143, p. 17360.
36. Redshaw, C. and Elsegood, M.R.J., *Angew. Chem., Int. Ed. Engl.*, 2007, vol. 46, p. 7453.
37. Mon, M., Lloret, F., Ferrando-Soria, J., et al., *Angew. Chem., Int. Ed. Engl.*, 2016, vol. 55, p. 11167.
38. Yang, F., Xing, Y., Deng, Z., et al., *Int. J. Chem. React.*, 2021, vol. 19, p. 1103.
39. Li, Y.-W., Zhao, J.-P., Wang, L.-F., and Bu, X.-H., *CrystEngComm*, 2011, vol. 13, p. 6002.
40. Zeng, M.-H., Feng, X.-L., and Chen, X.-M., *Dalton Trans.*, 2004, p. 2217.
41. Zorina-Tikhonova, E.N., Yambulatov, D.S., Kiskin, M.A., et al., *Russ. J. Coord. Chem.*, 2020, vol. 46, p. 75. <https://doi.org/10.1134/S1070328420020104>
42. Kiskin, M.A., Fomina, I.G., Aleksandrov, G.G., et al., *Inorg. Chem. Commun.*, 2004, vol. 7, p. 734.
43. Randall, C.R., Shu, L., Chiou, Y.-M., et al., *Inorg. Chem.*, 1995, vol. 34, p. 1036.
44. Krause, L., Herbst-Irmer, R., Sheldrick, G.M., and Stalke, D., *J. Appl. Crystallogr.*, 2015, vol. 48, p. 3.
45. Sheldrick, G.M., *Acta Crystallogr., Sect. C: Struct. Chem.*, 2015, vol. 71, p. 3.
46. Dolomanov, O.V., Bourhis, L.J., Gildea, R.J., et al., *J. Appl. Crystallogr.*, 2009, vol. 42, p. 339.
47. Çelenligil-Çetin, R., Staples, R.J., and Stavropoulos, P., *Inorg. Chem.*, 2000, vol. 39, p. 5838.
48. Cañada-Vilalta, C., Huffman, J.C., Streib, W.E., et al., *Polyhedron*, 2001, vol. 20, p. 1375.
49. Li, J., Zhang, F., Shi, Q., et al., *Inorg. Chem. Commun.*, 2002, vol. 5, p. 51.
50. Fukin, G.K., Samsonov, M.A., Baranov, E.V., et al., *Russ. J. Coord. Chem.*, 2018, vol. 44, p. 626. <https://doi.org/10.1134/S1070328418100020>
51. Fukin, G.K., Samsonov, M.A., Kalistratova, O.S., and Gushchin, A.V., *Struct. Chem.*, 2016, vol. 27, p. 357.
52. Grabowski, S.J., Dubis, A.T., Martynowski, D., et al., *J. Phys. Chem. A*, 2004, vol. 108, p. 5815.
53. Han, H., Wei, Z., Barry, M.C., et al., *Dalton Trans.*, 2017, vol. 46, p. 5644.
54. Dobrokhotova, Z., Emelina, A., Sidorov, A., et al., *Polyhedron*, 2011, vol. 30, p. 132.
55. Sapijanik, A.A., Kiskin, M.A., Kovalenko, K.A., et al., *Dalton Trans.*, 2019, vol. 48, p. 3676.
56. Gogoleva, N.V., Kuznetsova, G.N., Shmelev, M.A., et al., *J. Solid State Chem.*, 2021, vol. 294, p. 121842.

Translated by E. Yablonskaya